Comparative performance of coke oven gas, hydrogen and methane in a spark ignition engine

R. Ortiz-Imedio[1], A. Ortiz[1], J.C. Urroz[2], P.M. Diéguez[2], D. Gorri[1], L.M. Gandía[3], I. Ortiz[1]*

[1]Chemical and Biomolecular Engineering Department, University of Cantabria, Av. Los Castros 46, 39005, Santander, Spain

[2]Escuela Técnica Superior de Ingenieros Industriales y de Telecomunicación, Universidad Pública de Navarra, Campus de Arrosadía, E-31006 Pamplona, Spain

[3]Institute for Advanced Materials (InaMat), Public University of Navarre, Arrosadía Campus s/n, E-31006 Pamplona, Spain

*corresponding author: ortizi@unican.es

Abstract

In this study, coke oven gas (COG), a by-product of coke manufacture with a high volumetric percentage of H_2 and CH_4, has been identified as auxiliary support and promising energy source in stationary internal combustion engines. Engine performance (power and thermal efficiency) and emissions (NO_x, CO, CO_2 and unburned hydrocarbons) of COG, pure H_2 and pure CH_4 have been studied on a Volkswagen Polo 1.4 L port-fuel injection spark ignition engine. Experiments have been done at optimal spark advance and wide open throttle, at different speeds (2000-5000 rpm) and various air-fuel ratios (λ) between 1 and 2. The obtained data revealed that COG combines the advantages of pure H_2 and pure CH_4, widening the λ range of operation from 1 to 2, with very good performance and emissions results comparable to pure gases. Furthermore, it should be highlighted that this approach facilitates the recovery of an industrial waste gas.

Keywords

Internal combustion engine; coke oven gas; hydrogen; methane; spark ignition

1. Introduction

The dependence on fossil fuels in the main sectors of today's society has led to an unsustainable situation of greenhouse gas (GHG) emissions and pollution, causing a negative impact on natural resources and health of living beings [1]. To address this problem, among other strategies, different alternative fuels for internal combustion engines (ICE) are being investigated to decarbonize the transport sector and stationary engines field. Internal combustion engines are a very mature and well-established technology worldwide. These devices can be easily fed with unconventional liquid or gaseous fuels after making small preliminary modifications to withstand the different combustion conditions [2–7]. Hydrogen and methane fuel gases have received much attention over the last few decades due to their suitable characteristics as fuel gases in ICE. Many investigations have been conducted to study the influence of the composition of H_2 and CH_4 mixtures on various types of ICE: spark ignition (SI) [8–15], compression ignition (CI) [4,16–19] and homogeneous charge compression ignition (HCCI) [20–22], as well as of different configurations of fuel injection systems and experimental conditions.

Hydrogen, which is being promoted worldwide as an energy vector, offers clean combustion in terms of zero emissions of CO_2, CO, and hydrocarbons (HCs) [23–26]. However, its higher tendency to suffer from abnormal combustion phenomena and producing greater thermal NOx emissions, prevent from working at air-fuel (λ) ratios close to the stoichiometric one, and therefore, limit the power produced [27–30]. To avoid this limitation, hydrogen can be mixed with a proportion of methane, providing good knocking resistance, richer air-fuel mixtures and higher power performance [14,17,22,31–35]. However, the thermal efficiency, in-cylinder pressure and temperature, laminar flame speed and flammability limits are reduced as the methane content is increased [17,36,37]. In addition, the emissions of CO_2, CO and HCs, as well as the cyclic variations and combustion duration, are risen [22,38]. Just to show the influence of the mixture composition on the performance and pollutant emissions, some previous studies are mentioned below.

In the research conducted by Ma et al., (2007) [34], mixtures of H_2 and CH_4 with hydrogen fractions up to 50% were studied in a six cylinder diesel engine modified to work with a spark plug and a reshaped piston head to reduce the compression ratio. Experiments were carried out at 1200 rpm, manifold air pressure of 105 kPa, and one set of tests with a fixed spark timing of 30 degrees before top dead centre (dBTDC) and another set at optimum spark advance for maximum brake torque (MBT). With a fixed ignition timing, higher H_2 contents increased NOx emissions and there was no notable thermal efficiency improvement with rich air-fuel mixtures. However, at optimum spark advance, the NOx emissions of rich H_2 mixtures were lower compared to the first case, becoming negligible the influence of the H_2 content on the emissions, whereas higher efficiency was achieved with richer mixtures. HC emissions were reduced in both spark timing configurations.

In the study of Hora et al., (2015) [39], mixtures of hydrogen-enriched compressed natural gas (HCNG) containing between 0 and 30 vol% H_2 were tested in a port fuel single-cylinder spark ignition engine at 1500 rpm with a fixed spark ignition timing of 20 dBTDC. As the H_2 fraction and the load grew, the brake thermal efficiency increased and the specific consumption and HC, CO and CO_2 emissions were reduced. Furthermore, at low loads, the enrichment of H_2 increased the lean limit operation. However, the NO emissions rose with the H_2 fraction up to 20%, reaching stable values at different loads.

Experiments with hydrogen-mixtures containing up to 30 vol.% H_2 at wide open throttle (WOT), engine speeds between 1500 and 3000 rpm and λ ratios from 0.95 to 1.35 were carried out in a four-cylinder SI engine by Kahraman et al., (2009) [40]. Results in terms of in-cylinder pressure, thermal efficiency and HC, CO and CO_2 emissions were discussed. Higher H_2 content of the fuel increased the thermal efficiency and reduced HC, CO and CO_2 emissions. As the λ value rose, the peak pressure and CO and CO_2 emissions decreased. HC values showed a minimum at λ about 1.2, then increasing for higher air-fuel ratios due to a reduction of the mixture flammability.

On the other hand, Reyes et al., (2016) [41] focused on the analysis of the cycle-to-cycle variation when feeding mixtures of H_2 and CNG with H_2 fractions between 0 and 100% to a single-cylinder SI engine running at speeds between 1000 and

2500 rpm and fuel-air ratio of 0.7. A linear growth of the burning velocity was produced as the H_2 fraction increased. Moreover, the combustion variability was reduced when using mixtures containing above 25% of H_2.

In addition to the H_2-CH_4 mixtures, an interesting possibility is the use of already existing industrial surplus hydrogen streams, which can have two origins: i) production margin when the self-production exceeds the demand of the plant; ii) waste by-product coming from process industries that is not further used [42]. The first group of industries produce H_2 onsite and generate it in excess, and it is composed mainly of ammonia plants, oil refineries and methanol plants. As for the second group, H_2 is generated as by-product in ammonia purge gas streams, chlorine, ethylene and acetylene processes, and it is contained also in coke oven gas (COG) generated in coke manufacture [24,43]. A total potential between 2 and 10 billion Nm^3 of available surplus hydrogen in Europe has been statistically assumed: up to 5 billion Nm^3 from the first group of plants (i) and 2-5 billion Nm^3 as waste by-product (ii) [44].

Crude COG can be cleaned to extract valuable components such as tar, light oil (consisting mainly of BTX: benzene, toluene and xylene), sulphur and ammonia, and then, it can be used as fuel in metallurgical furnaces or as raw material in the chemical synthesis of methanol. Another option is the use of raw COG as heat source for the coking reactor with no further recovery steps [45]. However, COG is sometimes flared in periods of low energy consumption within the coke plant [43,46], reducing the global efficiency and wasting the valuable hydrogen energy content. COG can be used as fuel in stationary internal combustion engines coupled to the plants where it is produced due to its interesting composition and its high volumetric flow (280-450 Nm^3/h [45]) generated per ton of coke.

The typical composition of COG consists of around 90 vol% of combustible gases: 36-62% H_2, 16-35% CH_4 and 3-8% CO, and the rest are inert gases: 2-10% N_2, 1-5% CO_2 and small traces of other compounds [47,48].

Coke oven gas has been studied in previous works in both dual-fuel diesel engines [49,50] and spark ignition engines [51–55]. In the former types of engines, a pilot amount of diesel fuel is used to ignite the mixture by compression. Optimization of the equivalence ratio (inverse of λ) and the injection timing has

been conducted for different H_2 content gases [50], as well as the exhaust gas recirculation (EGR) ratio when using only COG [49]. Two-stage combustion results in maximum power output but is a precursor of knocking phenomena. Higher H_2 content in the fuel increases the thermal efficiency at the expense of generating lower power because the air-fuel ratio is increased to prevent knocking. In addition, EGR can increase the indicated mean effective pressure values and thermal efficiency, as well as reduce the NOx emissions.

In the case of SI engines, a synthetic gas mixture with a composition similar to that of COG was tested in a 0.825 L port-fuel single cylinder SI engine with a compression ratio (CR) of 10 at λ = 1 and 1500 rpm and the performance was compared with two synthesis gases with different compositions [52]. Results show good combustion stability and anti-knock properties of CH_4, CO and CO_2. A simpler gas composition of 65% H_2 and 35% CH_4 was tested in a 0.98 L engine of the same type with a CR of 9.7 varying λ from 1 to 1.5 and the EGR from 0 to 30% [53]. Knock reduction was achieved in a similar way by diluting the fuel mixture of the studied gas by means of EGR or by leaning the air-fuel mixture with an excess of air. A synthetic mixture composed of 55% of H_2 and 45% natural gas was used as a methanized coke oven gas and compared with natural gas and a mixture with 30% H_2 and 70% of natural gas in a turbocharged 6-cylinder SI engine [55]. The experiments were performed at 1200 rpm in two regimes: the former, with λ of 1.3 and varying the spark ignition timing from 0 to 40 dBTDC; the latter was conducted at a spark timing of 16 dBTDC varying λ from 1 to 2.4 at different loads. The methanized COG mixture presented higher efficiency and NOx emissions than the other fuels but producing lower torque and emissions of CO and HC; in addition, the optimum λ increased at higher load.

Recently, two works reporting modelling of SI engines fuelled with COG have been published [51,54]. The first work reports a detailed energy and exergy analysis for COG, CH_4 and syngas (80 vol% H_2 and 20 vol% CH_4) combustion [51]. The main conclusions highlighted the reduction of the irreversibility of COG when the CR or the throttle opening angle is increased and the ignition time is delayed, which improve the efficiency and reduce the specific fuel consumption (sfc). The second work is focused on obtaining a reduced and optimised mechanism for COG combustion; the kinetic model was coupled to computational

fluid dynamics (CFD) to simulate in-cylinder combustion with a reduction in the computational time [54]. Experimental in-cylinder pressures and NOx emissions are validated with the model at two crank angles showing a good concordance in the results.

The main purpose of this work is to investigate the use of hydrogen-rich waste streams such as COG in spark ignition engines at the industries where they are produced with the aim of e.g. generating electricity thus harnessing their energy content in a sustainable way. In this regard, the relevant operating parameters are the speed to produce an adequate frequency, which depends on the generator or the configuration of the system coupled; the efficiency; the power and the emissions generated. Many generator systems used in the industry produce electricity with a determined frequency according to the number of magnetic poles and the speed of the engine coupled; however, there are variable speed generator systems that allow working at optimal engine speed with higher efficiency and power and lower pollutant emissions maintaining the electricity frequency desired. This can be accomplished with power electronics or with devices, such as the Continuous Variable Transmission (CVT) [56,57].

In accordance with this fact, despite the interesting previous researches mentioned dedicated to studying coke oven gas (COG), to our knowledge, there is no a study on a mixture with the real composition of COG waste stream at different engine speeds and air-fuel ratio ratios to achieve optimal fuel combustion conditions. Therefore, the main novelty of this work is the use as fuel of a gas mixture typical a composition of COG waste stream that can be produced in a coke manufacture plant. The spark ignition engine was operated at wide open throttle (WOT) and optimum spark advance to obtain MBT, varying the air-fuel ratio and the engine speed to obtain optimum operating conditions. This study is aimed to help the interested industries to take advantage of this opportunity according to the internal combustion engine and generator system available to achieve efficient electricity generation with low pollutant emissions. To further understand the behaviour of COG waste stream composition and the benefits this fuel can provide, a comparison with pure H_2 and pure CH_4 gaseous fuels is carried out because they are the key components of COG. The study implied

analysing the performance of the fuels in terms of mean effective pressure, power, thermal efficiency, specific energy consumption and emissions produced.

2. Experimental setup and procedures

2.1 Test bench

The engine and the test bench used in this work have been adapted to work with gaseous fuels and have been described in detail in previous papers [3,31,58]. The ICE tested is a naturally aspirated four-cylinder Volkswagen Polo 1.4 L port fuel SI engine. A configuration of double overhead camshaft (DOHC) with four valves and a compression ratio of 10.5:1 is used. With gasoline feeding, the maximum brake power and MBT are 59 kW and 132 Nm at 5000 rpm and 3800 rpm, respectively.

The main modifications made to allow fuel gas feeding consisted of the integration of a metallic gas accumulator to maintain constant pressure, a cast manifold and gas injectors. The original electronic control unit was replaced by a programmable MoteC M 400 to calibrate the sensors and actuators, and a wideband lambda sensor Bosch LSU 4.9 was chosen for lean mixtures operation instead of the original lambda sensor. Lambda could be stablished with an error of ±0.7% for values close to stoichiometric conditions ($\lambda = 1$) and below ±3.0% for lean mixtures (λ above 1.7).

An eddy current dynamometer AVL 80 with a BME 300 control unit are used to control the torque, accelerator position and engine speed. Precisions for torque and engine speed were ±0.2% and ±1 rpm, respectively. The test bench includes a Bosch ETT 008.31 analyser for CO_2 (±0.1%), CO (±0.001%), HC (±2 ppm) measurement and a Horiba MEXA-720NOx for NOx (±2 ppm) quantification in the exhaust gases. Bronkhorst flow meters are used to measure the gas and air mass flow rates with a precision of ±0.5%. The data acquisition system (DAS) is based on three modules of a National Instruments Ni-CompacDAQ and is connected to a LabView program in a computer that collects and shows real-time information of the equipment.

2.2 Fuel Gases

In this work, pure hydrogen (≥ 99.8%), pure methane (≥ 99.5%) and a synthetic gas mixture of coke oven gas with the composition indicated in Table 1 have been purchased to Nippon Gases Spain.

Table 1. Composition of coke oven gas (COG) in percentage by volume and by weight used in this study

Composition	H_2	CH_4	CO	N_2	CO_2
vol%	57	30	6	5	2
wt%	11.6	48.5	16.9	14.1	8.9

Physicochemical properties of H_2, CH_4 and COG are listed in Table 2. As can be seen, the lower heating value (LHV) per unit mass of H_2 is much higher than the value of CH_4; however, LHV of COG is the lowest due to the 16.9 wt% of CO in the composition (Table 1), a component that barely contributes with a value of 10.1 MJ/kg [59]. On the other hand, LHV per unit volume or per mol decreases as the H_2 content increases because of the lower density. Low densities and volumetric LHVs of gases explain a decrease in power output compared to gasoline or diesel fuels due to the bigger space filled, resulting in less intake of fresh air and lower engine volumetric efficiency. This disadvantage can be compensated employing higher compression ratio, turbocharging and direct injection (DI) to increase the pressure of the fuel gases [36].

Table 2. Typical physicochemical properties of H_2, CH_4 and COG calculated at 273.15 K and 10^5 Pa

Gas	H_2	CH_4	COG
LHV (MJ/kg)	120.00 [59]	50.00 [59]	39.86
LHV (kJ/mol)	241.91	802.12	395.50
LHV (MJ/m^3)	9.92	32.91	16.23
Density (kg/m^3) at STP	0.08	0.66	0.41
Molecular weight (g/mol)	2.02 [59]	16.04 [59]	9.92
Stoichiometric ratio (λ_{st})	34.21	17.20	12.72
Flammability range (vol%)	4.0 - 75.0 [60]	5.3 - 15.0 [60]	4.4 - 34.0 [48]
Laminar flame speed (m/s)	2.65 - 3.25 [61]	0.38 [61]	0.68 - 0.88 [51,62]

STP means standard temperature (273.15 K) and pressure conditions (10^5 Pa) according to IUPAC [63].

The general reaction for the complete combustion of 1 mol of COG for a given value, λ, of the air-fuel ratio is as follows (Eq. 1):

$$\begin{aligned} &\alpha CH_4 + \beta H_2 + \gamma CO + \delta CO_2 + \varepsilon N_2 + \left(2\alpha + \frac{\beta}{2} + \frac{\gamma}{2}\right)\lambda\left(O_2 + \frac{79}{21}N_2\right) \\ &\quad \rightarrow \quad (\alpha + \gamma + \delta)CO_2 + (2\alpha + \beta)H_2O + \left(2\alpha + \frac{\beta}{2} + \frac{\gamma}{2}\right)\lambda\frac{79}{21}N_2 + \varepsilon N_2 \\ &\quad + (\lambda - 1)\left(2\alpha + \frac{\beta}{2} + \frac{\gamma}{2}\right)O_2 \end{aligned} \tag{1}$$

The parameters α, β, γ, δ and ε are factors multiplying the stoichiometric coefficients that correspond to the volumetric percentages of the composition of COG shown in Table 1. Stoichiometric air-fuel ratio (λ_{st}) of the gases are calculated according to the general reaction giving a null value for the parameters of the components not found in the fuels in the case of pure gases. With the molecular weight of air (28.966 g/mol for dry air) and each gas, the mass flows (g/s) are calculated and Eq. 2 is applied.

$$\lambda_{st} = \frac{\dot{m}_{air}}{\dot{m}_{fuel}} \tag{2}$$

The flammability limits are the range of fuel-air mixtures compositions, in percentage by volume, in which they are able to ignite and propagate in a self-sustained way. The range of H_2 is far wider compared to CH_4. The COG upper flammability limit is almost half of the H_2 due to the high volume content of hydrogen in the mixture.

Laminar flame speed (S_L) is a characteristic of the air-fuel chemical reactivity, combustion enthalpy and physical diffusivity, influencing the rate of heat release rate in SI engines. S_L strongly rises with the increase of H_2 percentage in the fuel composition enhancing the mixture chemical reactivity by increasing the concentration of H, O and OH radical species. This trend is linear up to 50% of H_2 with a slight increase due to the less-reactive component, CH_4. From 50% to 90% of H_2, there is an exponential increase in S_L, ascending finally very rapidly in the range 90-100%. This non-linear behaviour caused by the contribution of

the slowly reacting methane affects strongly to the chemical kinetics and the flame propagation process [36,64,65].

2.3 Experimental methods

The study of pure H_2, pure CH_4 and synthetic COG has been conducted through experiments at a wide speed range from 2000 to 5000 rpm and WOT for full load with maximum air inlet flow (Table 3). The spark advance was selected in order to obtain the MBT in each working condition. The λ range was varied between 1 and 2. However, λ values for H_2 were set at 1.5 and 2 to avoid the risk of combustion anomalies such as pre-ignition, backfire and knocking with fuel-rich mixtures [66]. λ is limited to 1 and 1.5 for CH_4 due to poor combustion at leaner compositions increasing emissions of unburnt methane. On the other hand, COG combines the advantages of both pure fuel gases extending the range of operation from 1 to 2. The good knocking resistance of CH_4 allowed the reduction of air-fuel ratio for COG without abnormal combustion phenomena except at 5000 rpm for λ = 1. The wider flammability range of H_2 component enabled the burning of the fuel gas at lean λ ratio.

For the experiments with COG (λ = 1.5) at 5000 rpm and COG (λ = 1) at the whole range of engine speeds, the fuel gas injection pressure was increased to 4 bar instead of 3 bar used in the rest of the experiments, because the gas injectors were not able to inject the required fuel volume at the set speed. Even though, the engine was able to reach stoichiometric λ conditions up to 4000 rpm.

Table 3. Experimental tests conditions

Fuel	λ	Speed (rpm)	Spark advance	Load
H_2	1.5 , 2	2000 – 5000	Optimum	WOT
CH_4	1 , 1.5	2000 – 5000	Optimum	WOT
COG	1 , 1.5 , 2	2000 – 5000	Optimum	WOT

3. Results and discussion

The performance of the ICE was tested in terms of brake mean effective pressure (BMEP), power, thermal efficiency (η_t) and specific energy consumption (SEC)

for each gas. On the other hand, emissions of NOx, HC, CO and CO_2 were collected at the engine exhaust, analysed, and calculated per energy unit (g/kWh) to normalize the results.

3.1 Engine performance

The performance comparison of the three gases has been carried out at optimum spark advance and WOT to achieve the MBT, and hence, the highest power values at each test condition. Fig. 1 shows the ignition advance in dBTDC for pure H_2, pure CH_4 and COG varying the engine speed between 2000 and 5000 rpm and λ values between 1 and 2. COG with λ = 1 only reached 4000 rpm due to abnormal combustion at higher speeds.

As the H_2 concentration in the fuel increases, the ignition (spark) advance angle decreases because of higher S_L and therefore, improved mixture chemical reactivity and lower combustion duration [60,67]. This effect can be observed through the lower advance of pure H_2 and COG compared to pure CH_4. Also, COG requires a higher spark advance than pure H_2 at the same λ due to the presence of inert gases, as well as CO and CH_4 (Table 1). In addition, lean air-fuel mixtures (high λ) entail increased ignition advance to burn the high air percentage in the combustion chamber [3].

In general, at low speeds, the required ignition advance angle becomes lower because there is a longer period of time available to burn the air-fuel mixture, meanwhile at higher speeds, the period of time available for the same angle is lower, requiring a higher spark advance to compensate this fact.

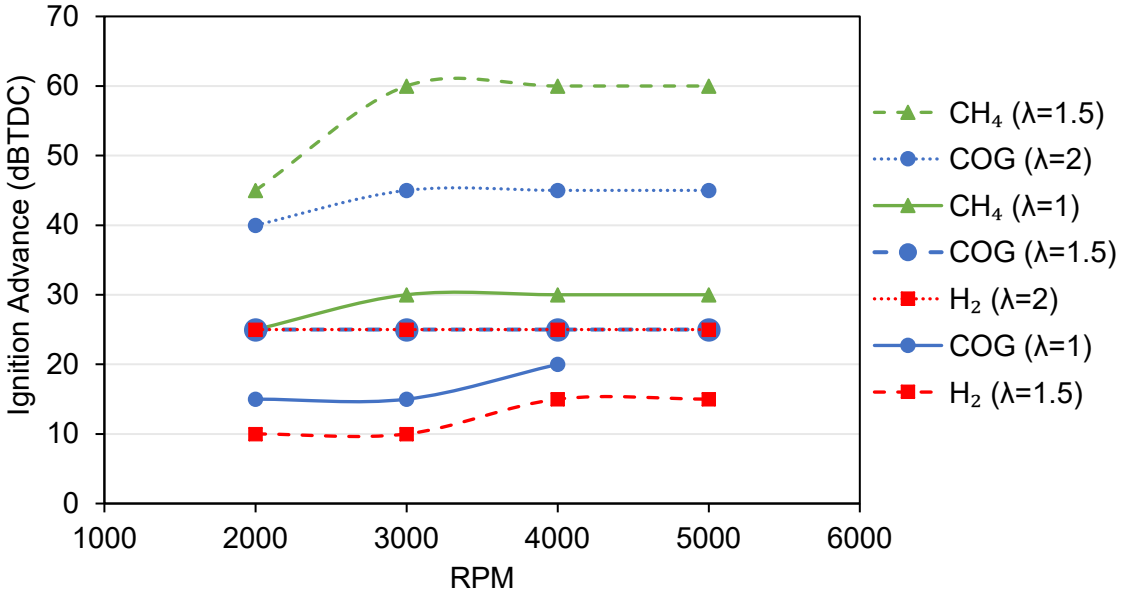

Fig. 1 – Ignition advance angle (dBTDC) versus engine speed (rpm) of H_2 (red squares), CH_4 (green triangles) and COG (blue dots) at WOT and different λ values

To assess the performance, the BMEP parameter (in kPa) is typically used, which removes the dependency on engine size by dividing the work obtained per cycle by the cylinder volume displaced (V_d, in m^3), and is calculated with Eq. 3 [59].

$$BMEP = 60 \cdot \frac{P \cdot n_R}{V_d \cdot N} \tag{3}$$

Where P (kW) is the power generated, n_R is the number of revolutions per cycle (with a value of 2 for a four-stroke engine) and N (rpm) is the engine speed.

Fig. 2 shows the engine BMEP when using the three fuels under study versus the engine speed at the different λ conditions and WOT. For λ values higher than 1, COG provides greater BMEP than pure H_2 and pure CH_4, thanks to an adequate trade-off between higher volumetric LHV (16.23 MJ/m^3) than H_2 (9.92 MJ/m^3), and higher S_L than CH_4. With λ = 2, the difference between COG and H_2 is very small, possibly due to the diluent effect of air. However, at λ = 1 the performance of pure CH_4 prevails over COG because the latter has a high composition in weight percentage of inert gases, N_2 and CO_2, decreasing the LHV and the effective power, and therefore, reducing the η_t of the engine. Comparing H_2 and CH_4, at λ = 1.5, the former gas supplies higher BMEP taking advantage of the higher S_L and the wider flammability range.

The increase of H_2 content in the fuel provides a more stable combustion, decreasing the variation of the BMEP values throughout the range of speeds [68]. For COG and CH_4 in every λ condition, the maximum BMEP value is reached at 4000 rpm, meanwhile, for pure H_2 the greatest BMEP is at 5000 rpm.

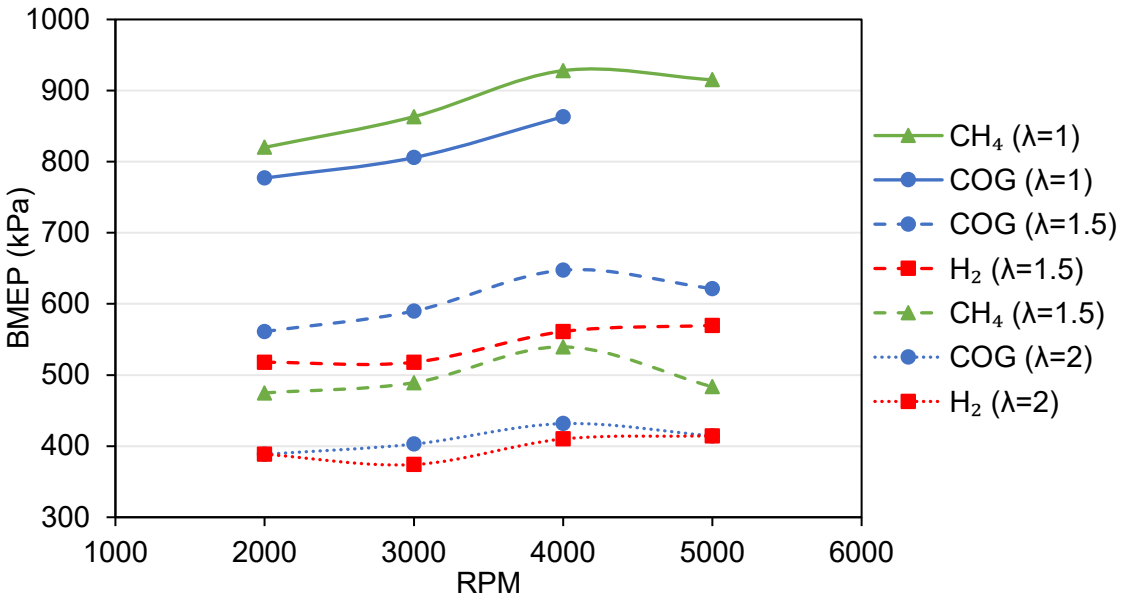

Fig. 2 – BMEP (kPa) versus engine speed (rpm) of H_2 (red squares), CH_4 (green triangles) and COG (blue dots) at WOT and different λ values

If the engine power with the three gases at different engine speeds and varying λ is considered (Fig. 3), the important effect of the λ ratio on the power can be highlighted. As the mixture becomes leaner, the power decreases due to the excess of air which reduces the combustion temperature and the heat released.

At λ = 1, CH_4 prevails over COG on the whole range of speeds, increasing the difference as the engine speed rises. In the case of λ = 1.5, COG dominates over pure H_2 and pure CH_4 at each engine speed, especially in the high part of the range. However, H_2 performs similar to CH_4 at that air-fuel ratio, except in the case of 5000 rpm, where the power difference increases due to the steeper slope of CH_4 at that speed. On the other hand, at λ = 2, COG power results are very similar to pure H_2, widening the difference at medium speeds.

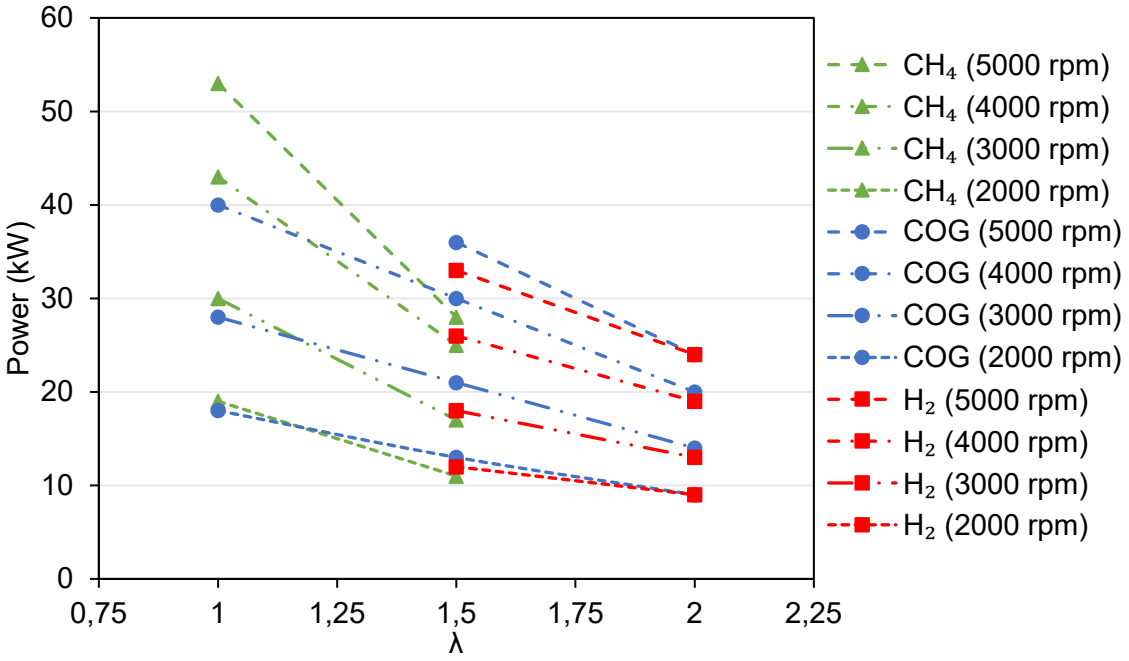

Fig. 3 – Power (kW) versus air-fuel ratio (λ) of H_2 (red squares), CH_4 (green triangles) and COG (blue dots) at different engine speed values and WOT

Thermal efficiencies of the three gases under consideration are shown in Fig. 4.

The η_t parameter relates the ratio of the power obtained and the energy of the fuel required. As the power delivered increases with a determined quantity of fuel energy, the efficiency rises. In addition, for a constant power generation, a lower volumetric LHV increases η_t because the fuel can provide the same amount of power with a lower energy content.

In this case, comparing the three gases at λ = 1.5 and 4000 rpm, efficiency increases of 7.0% and 10.3% are obtained with COG compared to pure H_2 and pure CH_4, respectively. Although the volumetric LHV of COG is an intermediate value between those of CH_4 and H_2, the power (and hence, BMEP) achieved is higher at that λ (Fig. 2), predominating in the ratio of the thermal efficiency. Comparing H_2 and CH_4 at λ = 1.5, the former has lower volumetric LHV and higher power is achieved than with the latter, following the trend explained previously. Despite the fact that a lower power value is achieved at λ = 1 with COG and CH_4 (Fig. 2), the first one has the half value of LHV by volume (Table 2), predominating in a significant way in the thermal efficiency. In the case of λ = 2 with H_2 and

COG, H_2 has lower volumetric LHV than COG but also the power obtained is below, reducing η_t.

Considering each fuel individually, lower air-fuel ratios lead to greater η_t because the power delivered increases significantly while the fuel energy required rises in a minor proportion. However, there is an exception for COG, providing the maximum η_t at λ = 1.5 and decreasing for richer mixtures (λ = 1) due to incomplete combustion because there is less oxygen available in the combustion chamber [32,69–71]. With fuel lean mixtures (high λ values) the efficiency also decreases due to less stable combustion [32,67,70].

Regarding the effect of the engine speed, the maximum efficiency is achieved at 4000 rpm for all the gases except in the case of CH_4 (λ = 1), that is reached at 5000 rpm. This dependence of the thermal efficiency on the engine speed can be harnessed by the industries interested on using the clean COG waste stream in ICEs to generate electricity coupling the engine to the generator with systems like power electronics or CVT systems [56,57]. These devices allow maintaining constant the current frequency produced and at the same time use the engine at optimal conditions with higher power output and lower fuel consumption.

In the case of H_2, a small variation of the η_t curves is observed throughout the whole range of engine speeds, revealing higher combustion stability due to complete combustion, in good accordance with the literature [37,68].

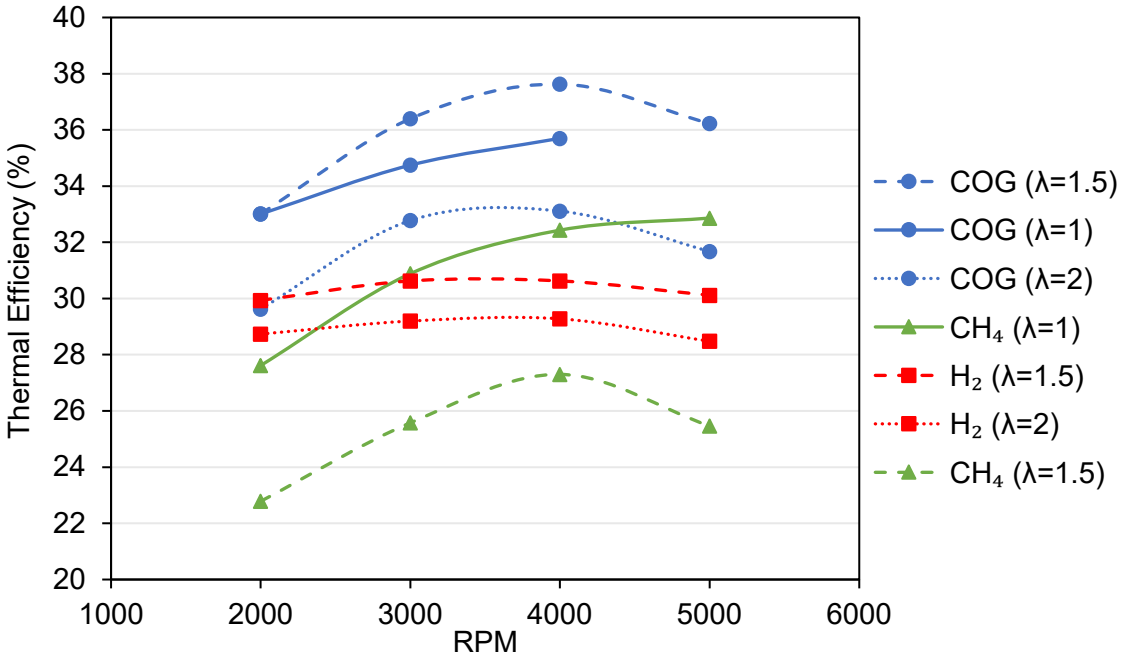

Fig. 4 – Thermal efficiency versus engine speed (rpm) of H_2 (red squares), CH_4 (green triangles) and COG (blue dots) at different λ values

In Fig. 5 the specific energy consumption (SEC, in MJ/kWh) is plotted at WOT and different λ values varying the engine speed. The SEC represents the amount of total fuel energy that is needed to produce 1 kW of power during 1 h of operation in the engine [4]. An inverted relationship can be observed between the thermal efficiency and SEC curves, following the same trends.

As the volumetric LHV of the fuel increases, the SEC value rises because the fuel provides higher energy and more energy is consumed per cubic meter of fuel injected. For that reason, H_2, with a very low volumetric LHV due to its low density, occupies more volume in the combustion chamber but provides less energy, reducing the SEC value with respect to CH_4 at λ = 1.5, which has higher volumetric LHV. On the other hand, COG at λ = 1.5, with an intermediate value of LHV, should be in the middle of both pure gases, but as this gas can deliver more power (and therefore, BMEP) than H_2 (Fig. 2), the SEC is reduced. If CH_4 and COG are compared at λ = 1, methane gets closer to COG curve as the power delivered by the former is greater than the latter, however, the lower volumetric LHV of COG (the half than CH_4) prevails, reducing its SEC value. In contrast, in the case of λ = 2, although COG has higher volumetric LHV than H_2, COG delivers more power, predominating in this case.

Considering each fuel individually, as the λ ratio increases, the SEC value increases as well because the fuel mixture becomes leaner. Although lower fuel volume is injected at higher λ, the power is reduced significantly, and therefore, more energy of the fuel is required per unit of mechanical energy delivered. However, in the case of COG, the minimum SEC values are obtained at λ = 1.5 and increase at richer mixtures because there is less oxygen available with λ = 1, causing incomplete combustion and more fuel is consumed to give the same amount of mechanical energy.

Regarding the effect of the engine speed, the minimum SEC value is reached at 4000 rpm for all the gases except in the case of CH_4 (λ = 1), achieved at 5000 rpm. This effect is the opposite of the one commented for η_t. Furthermore, as mentioned before (Fig. 4), the higher combustion stability of H_2 in the whole range of speeds is also proven in the almost constant values of SEC, with a variation around only 3% between the lowest and highest values.

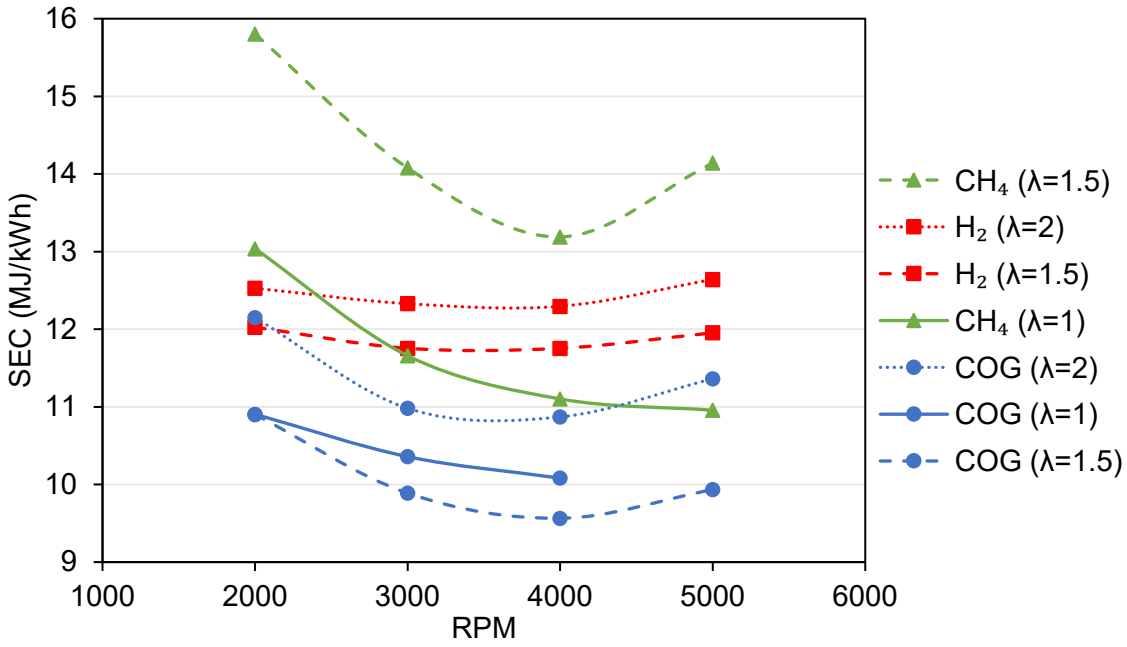

Fig. 5 – Specific energy consumption (SEC, in MJ/kWh) versus engine speed (rpm) of H_2 (red squares), CH_4 (green triangles) and COG (blue dots) at different λ values

With the analysis of the performance results carried out, the importance of the air-fuel ratio and the engine speed working at MBT and WOT is highlighted, obtaining for this engine the greatest BMEP value at λ = 1 and 4000 rpm for COG.

However, higher thermal efficiency and lower SEC are achieved at λ = 1.5 and 4000 rpm. Therefore, the industry users interested in using this waste stream in ICEs, have the option of working at higher power values or with higher efficiency performance reducing the fuel consumption. In these cases, to operate at a speed different than the one used with conventional generators, a power electronics system or a CVT device is necessary to adapt the engine speed chosen to the desired electricity frequency given as output by the generator.

3.2 Emissions

Once the performance of the combustion of the gaseous fuels has been described, the specific NOx, HC, CO and CO_2 emissions are discussed in what follows. Specific emissions were calculated according to Eq. 4 (written for the case of NOx) [31].

$$sNO_x = \frac{60 \cdot 10^{-6}}{V_m} \cdot \frac{\dot{V}_f \cdot N_e \cdot M_{NO_x} \cdot C_{NO_x}}{P} \quad (4)$$

Where the specific emissions of NOx (sNOx) are in g/kWh, V_m is the molar volume (22.71 L/mol at STP conditions), $\dot{V}_f$ (NL/min) is the fuel flow rate, N_e are the exhaust moles formed assuming complete combustion of 1 mol of fuel with Eq. 1, M_{NO_x} (g/mol) is the molecular weight of the gas (assumed as 30 g/mol considering the main product is NO), C_{NO_x} (ppm) is the concentration of NOx in the exhaust and P (kW) is the brake power generated. For HC, CO and CO_2 pollutants, the exhaust measurements have been done on dry gases and the exponent “-6” in Eq. (4) is changed to “-2” because they are measured in “%” instead of “ppm”.

The sNOx measured in the exhaust are shown in Fig. 6. These emissions depend mainly on the temperature reached during combustion and the concentration of the reactants (N_2 and O_2) in the air-fuel mixture, as it is well known with the extended Zeldovitch model [31]. The experiments carried out in the literature show that in the case of working at constant spark timing, the sNOx emissions are increased with higher H_2 content in the mixture at same λ value [27,31,34,39,73]. However, if the spark timing is selected in order to obtain the MBT, the specific NOx emissions are similar or even lower with higher H_2

contents at same λ value and speed than leaner mixtures [31,34]. With high H_2 contents, the optimum ignition timing is retarded (Fig. 1), reducing the work in the compression stroke and decreasing the combustion temperature, and hence, reducing NOx emissions. Hoekstra et al., (1996) [73] and Shudo et al., (2000) [74] also prove that as the ignition timing is delayed, the NOx emissions are reduced. Therefore, a trade-off between higher NOx emissions with higher H_2 contents and reduced emissions due to the ignition timing delayed is produced in the experiments carried out in this study. As the ignition timing of pure H_2 with λ = 1.5 is significantly delayed for MBT (10º at 2000 and 3000 rpm and 15º at 4000 and 5000 rpm), the NOx emissions have similar values than with CH_4, which is ignited with a very advanced spark timing (45º at 2000 rpm and 60º at higher speeds). On the other hand, COG presents lower NOx values at all λ values because this gas incorporates both benefits commented: lower H_2 content than pure H_2, and higher ignition timing delay than pure CH_4.

As can be observed from each gas independently, fuel-rich mixtures (low λ values) favour NOx generation due to the dominant effect of temperature, however, at λ values close to 1, the O_2 concentration is small, limiting the NOx formation [32]. There is an exception for the case of CH_4 at low engine speeds, probably because the power delivered is not so great and the fuel consumption is still high, increasing the ratio between emissions and power produced.

With lean mixtures (high λ values), the NOx emissions drop due to the excess air in the cylinder, reducing the combustion temperature [72]. COG (λ = 2) delivers the lowest NOx emissions due to the important content of no H_2 components in its composition and the dilution effect of air, decreasing the temperature during the combustion and hence, the thermal NOx formation. The greatest influence of λ in sNOx values is observed for pure H_2; thus, in H_2 engines, limiting the combustion temperature by air dilution would be an interesting strategy to reduce NOx emissions.

This trade-off between low O_2 concentration and reduced combustion temperature at low and high λ values, respectively, explains the higher emissions of COG combustion at intermediate λ values (1.5) than at λ = 1, achieving better combustion.

The minimum emissions are achieved at 3000 rpm for almost all the gases and test conditions. At higher speeds, better turbulence favours a greater mixture in the combustion chamber, and therefore, higher NOx emissions due to better combustion phenomena [75].

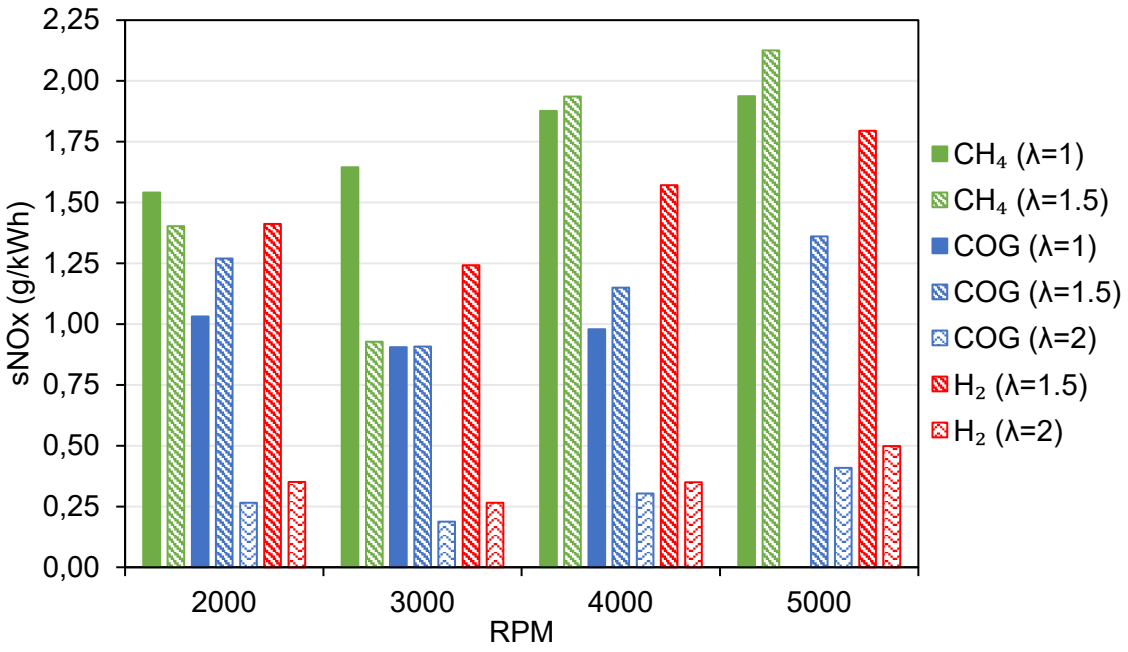

Fig. 6 – Specific NOx emissions (sNOx, in g/kWh) versus engine speed (rpm) of CH_4, COG and H_2 at different λ values

Fig. 7 shows the evolution of the specific hydrocarbons emissions (sHC, in g/kWh) at different λ values across the speed range tested. HC emissions are mainly produced because of incomplete combustion caused by quenching of the flame near the cylinder walls or due to local air-fuel inhomogeneity, as well as from unburned fuel trapped in crevices not reached by the flame, emitting unburned hydrocarbons [76]. At λ values above 1 but close to the unit, there is an extra air condition which assures complete combustion and the mixture is not too lean, allowing a high exhaust temperature and hence, oxidizing the HC formed through crevice and flame quenching [34]. As the air-fuel mixture becomes leaner (high λ values), the flammability of the mixture is reduced and sHC rise. This effect can be clearly observed for CH_4 and to a lesser extent for COG. The former case can be explained because the flammability range of CH_4 is lower than for pure H_2 and COG, resulting in very poor combustion when the air excess increases, raising the emissions very steeply. In the case of COG, as

the flammability range is wider, the mixture can still burn properly with λ = 1.5, although at higher λ values, sHC emissions strongly rise as well [77]. The same trend can be observed in Ma et al., (2007) [34], increasing the emissions in a steeper way with richer fuel mixtures in the case of pure CH_4, and delaying the effect to leaner mixtures when the hydrogen fraction increases.

In addition, as COG is enriched with H_2, the fuel carbon content is lower, the quenching distance is smaller and the combustion temperature is higher, reducing the sHC emissions, as can be observed in the comparison between CH_4 and COG [78].

The sHC emissions decrease with the rise of engine speed thanks to the improved fuel combustion due to a better mixing associated with more intense turbulence inside the cylinder. However, the emissions of CH_4 (λ = 1.5) rise again at 5000 rpm because the power decreases steeply from λ = 1 to λ = 1.5 and the thermal efficiency also drops rapidly at that engine speed, as can be seen in Fig. 3 and Fig. 4.

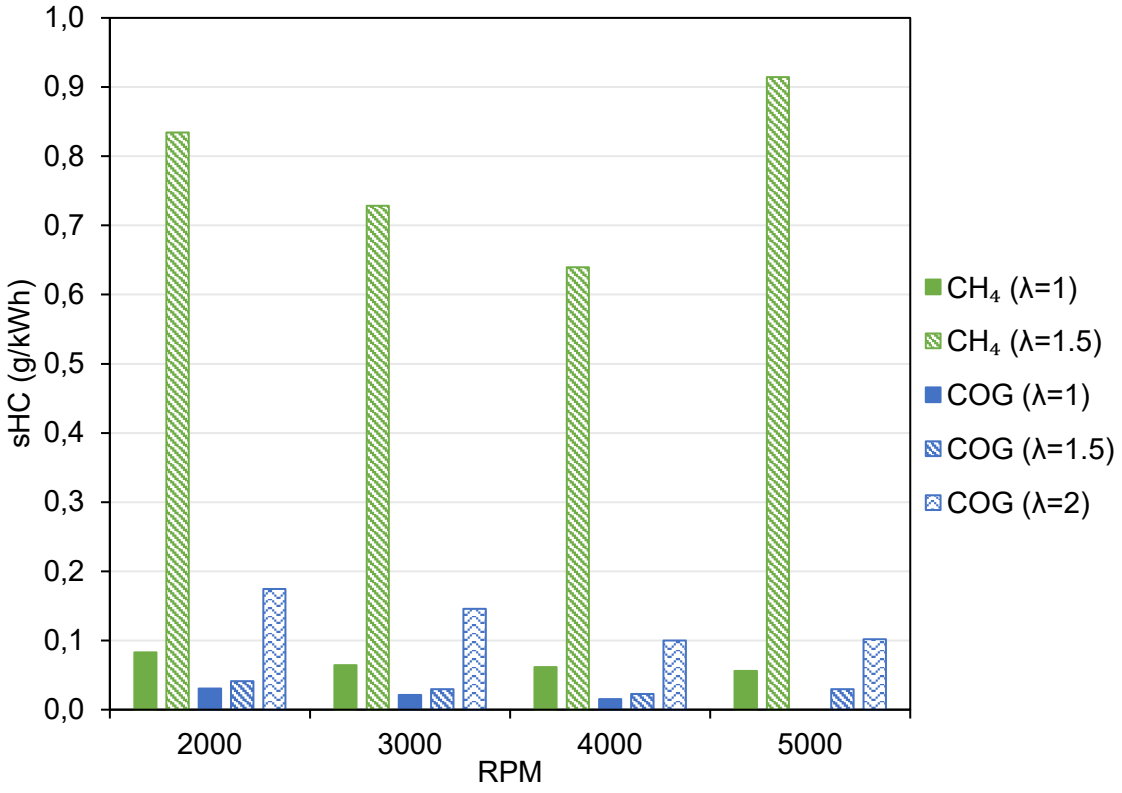

Fig. 7 – Specific hydrocarbons emissions (sHC, in g/kWh) versus engine speed (rpm) of CH_4 and COG at different λ values

Fig. 8 depicts the specific carbon monoxide emissions (sCO, in g/kWh) of the engine exhaust for selected λ values in the experiments performed with CH_4 and COG between 2000 and 5000 rpm and full load. As COG includes a fraction of CO in its composition, it has a higher tendency to emit carbon monoxide in the case of incomplete combustion. On the other hand, hydrogen enrichment helps to reduce the sCO emissions, as it can be observed in the comparison between CH_4 and COG, by increasing the combustion temperature and the concentration of OH radicals, which promote the oxidation of CO to CO_2 [79]. The highest CO emissions are produced with CH_4 (λ = 1) because CO is formed as an intermediate product of CH_4 oxidation when the O_2 available in the air-fuel mixture is low, limiting the complete combustion in the cylinder to form CO_2 [76]. With a leaner mixture in both fuels (λ = 1.5), the increase of O_2 content is beneficial to reduce the sCO emissions drastically, promoting a more complete combustion [80]. The same trend is observed in Açikgöz et al., (2015) [81] and in Ma et al., (2007) [34], increasing the CO emissions as the excess air ratio approaches to stoichiometric conditions. However, at even leaner mixtures in the case of COG (λ = 2), although the carbon content in the air-fuel mixture is lower, the sCO values rise again because a more unstable combustion, lower combustion temperature reducing oxidation rates and a higher probability of large-scale flame quenching, limiting the complete oxidation of the fuel and then increasing sCO [32,34,76,82]. In addition, the reduction of the generated power at this condition is more pronounced than the sCO emissions produced [31,78].

In general, as the engine speed increases, the emissions are reduced because the increased turbulence inside the cylinder favours the combustion, except in the case of CH_4 (λ = 1), with a minimum at 3000 rpm. This can be explained because the air-fuel mixture is so rich that at higher engine speeds, the available time to complete the combustion is lower leading to increased emissions.

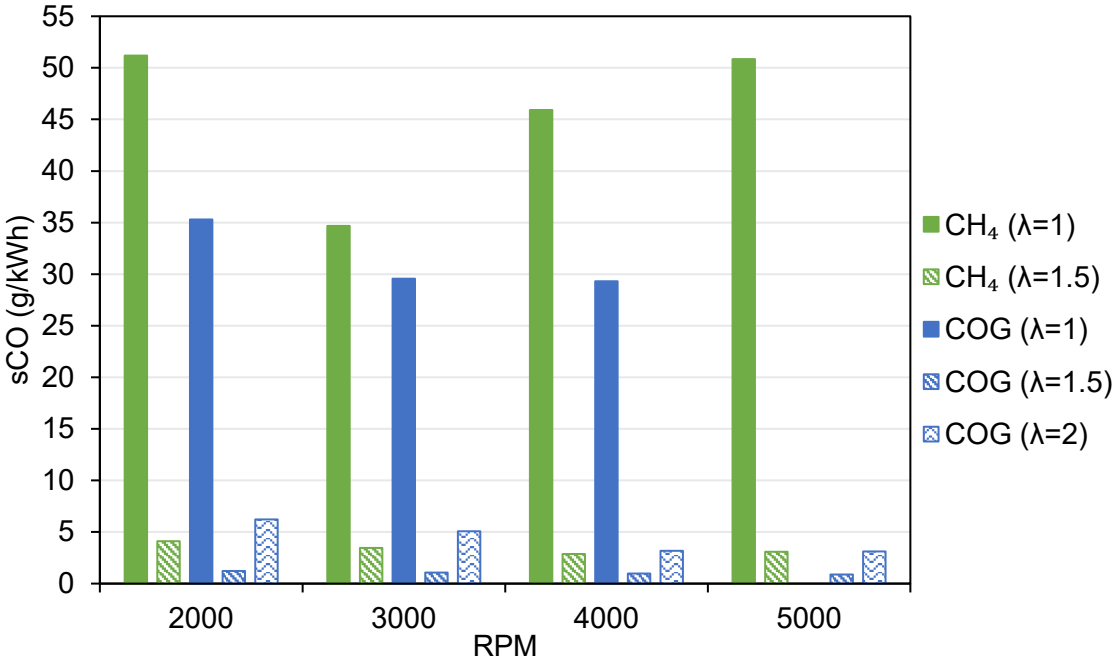

Fig. 8 – Specific carbon monoxide emissions (sCO, in g/kWh) versus engine speed (rpm) of CH_4 and COG at different λ values

Finally, the specific emissions of carbon dioxide (sCO_2, in g/kWh) are graphed in Fig 9. These emissions arise as products of the complete combustion of a hydrocarbon fuel.

In contrast to the other pollutants, the influence of λ and the engine speed on sCO_2 emissions is very small. Generally, with rich mixtures, the specific CO_2 emissions decrease because of a limited oxygen availability. Moreover, with very lean mixtures the CO_2 emissions also decrease because the carbon content is reduced and the combustion is poor [78]. However, at medium λ values (1.5), CO_2 emissions increase because the efficiency is higher, and the oxygen concentration is adequate to achieve complete combustion. Considering specific emissions, the same reasoning can be applied, nevertheless, the power reduction with lean mixtures is more pronounced than the emissions generated, raising the sCO_2 values, especially at higher engine speeds [27,78].

On the other hand, the H_2 fraction on the fuel composition of COG has a clear effect on sCO_2, which decrease as the H/C ratio of the mixtures increases. It should be noted that COG has typically a little fraction of CO_2 in its composition,

which is an inert gas as concerns combustion, and therefore, it has a direct contribution to the carbon dioxide emissions.

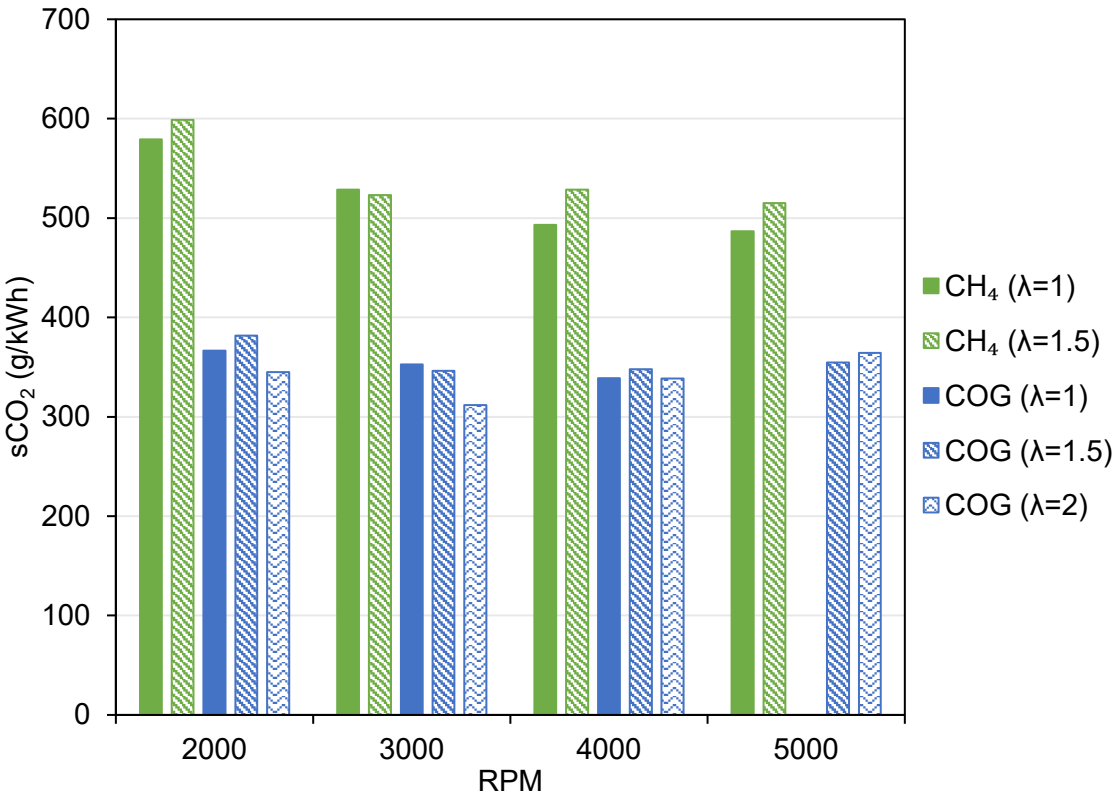

Fig. 9 – Specific carbon dioxide emissions (sCO_2, in g/kWh) versus engine speed (rpm) of CH_4 and COG at different λ values

In summary, considering the emissions results of COG, this waste stream can be operated in this engine at λ = 2 to obtain lower values of sNOx and sCO_2 but with higher amount of sHC and sCO than working at λ = 1.5. Regarding the engine speed, operating at 3000 rpm reduces the emissions of sNOx and sCO_2 but increases slightly the sHC and sCO values compared to 4000 rpm.

Conclusions

A comparative experimental study of pure H_2, CH_4 and COG gaseous fuels in a Volkswagen Polo 1.4 L port-injection SI engine has been developed. Experiments were carried out at full load (WOT) and optimal spark advance to obtain MBT. λ values between 1 and 2 were selected varying the engine speed between 2000 and 5000 rpm. The main conclusions regarding the comparisons of the three gases are summarized as follows.

- For λ values higher than 1, COG provides greater BMEP and power than pure H_2 and pure CH_4, due to the favourable influence of the higher LHV of COG in comparison to H_2 and higher S_L value compared to CH_4. With leaner mixtures, the BMEP and power decrease, being this reduction more pronounced at high speeds.
- COG delivers the greatest η_t values. At λ = 1.5, a η_t increase of 7.0% and 10.3% were obtained with COG with respect to H_2 and CH_4 in the maximum values, respectively. Fuel gases with lower LHV by volume reduce the SEC. SEC values increase at high λ values due to a reduction in η_t, except COG (λ = 1) that reaches the maximum η_t at λ = 1.5.
- The delayed spark timing operating at MBT with fuels with high H_2 percentage can reduce sNOx due to lower combustion temperature. COG presents lower values because of lower H_2 content and higher spark timing delay than CH_4. Very low and very high λ values reduce the O_2 concentration and the temperature, respectively, reducing sNOx.
- The flammability of the mixture is reduced with high λ values and the sHC emissions rise. By enriching the fuel with H_2, the fuel carbon content is lower, the quenching distance is smaller, and the combustion temperature is higher, reducing sHC emissions.
- The highest sCO emissions are produced with CH_4 (λ = 1) because the O_2 available is low. At lean mixtures (λ = 2) the sCO values rise again because of a more unstable combustion.
- sCO_2 emissions rise with intermediate λ values due to better combustion and decrease as the H/C ratio of the mixture increases.
- The major strength of COG is the combination of advantages of pure H_2 and pure CH_4, widening the λ range of operation from 1 to 2, with very good performance and emissions results comparable to pure gases.

These results reveal COG as a very good fuel for ICEs. This gas comes from an industrial waste stream and can be applied in stationary engines coupled to generator systems with power electronics or CVT systems to work at optimal conditions while maintaining the electricity frequency desired. The optimum conditions for using COG in the engine employed in this work were with λ = 1.5 at 4000 rpm achieving high power performance and η_t, the lowest SEC, moderate

NOx and CO_2 emissions, and small values of sHC and sCO. At 3000 rpm or λ = 2, lower values of sNOx can be achieved but the combustion performance and efficiency are reduced. Another way to reduce the emissions is by incorporating a three-way catalytic converter (TWC) in the exhaust. Thus, the operating conditions should be optimized for each engine and the purpose of the application.

Acknowledgements

This research is being supported by the Project “HYLANTIC”- EAPA_204/2016, which is co-financed by the European Regional Development Fund in the framework of the Interreg Atlantic program. Rafael Ortiz-Imedio thanks the Concepción Arenal postgraduate research grant from the University of Cantabria.

Nomenclature

COG	coke oven gas
BMEP	brake mean effective pressure
CA	crank angle
CFD	computational fluid dynamics
CI	compression ignition
C_{NO_x}	concentration of NOx in the exhaust
CNG	compressed natural gas
CR	compression ratio
CVT	continuous variable transmission
dBTDC	degrees before top dead centre
DME	dimethyl ether
DOHC	double overhead camshaft
EGR	exhaust gas recirculation
GHG	greenhouse gas emissions
HCCI	homogeneous charge compression ignition

HCNG	hydrogen enriched compressed natural gas
ICE	internal combustion engine
LHV	lower heating value
MBT	maximum brake torque
$\dot{m}_{air}$	mass flow rate of air
$\dot{m}_{fuel}$	mass flow rate of fuel
M_{NO_x}	molecular weight of NOx
N	engine speed
N_e	exhaust moles with complete combustion
n_R	revolutions per cycle
P	power
SEC	specific energy consumption
sfc	specific fuel consumption
SI	spark ignition
S_L	laminar flame speed
sNOx	specific NOx emissions
STP	standard temperature and pressure (273.15 K and 1 bar)
TDC	top dead center
TWC	three-way catalytic converter
V_d	displaced volume
$\dot{V}_f$	fuel flow rate
V_m	molar volume
WOT	wide open throttle
λ	air-fuel ratio
λ_{st}	stoichiometric air-fuel ratio
η_t	thermal efficiency

References

[1] Dincer I, Zamfirescu C. Chapter 2 – Hydrogen and Its Production. Elsevier; 2016. https://doi.org/10.1016/B978-0-12-801563-6.00002-9.

[2] Escalante Soberanis MA, Fernandez AM. A review on the technical adaptations for internal combustion engines to operate with gas/hydrogen mixtures. Int J Hydrogen Energy 2010;35:12134–40. https://doi.org/10.1016/j.ijhydene.2009.09.070.

[3] Sopena C, Diéguez PM, Sáinz D, Urroz JC, Guelbenzu E, Gandía LM. Conversion of a commercial spark ignition engine to run on hydrogen: Performance comparison using hydrogen and gasoline. Int J Hydrogen Energy 2010;35:1420–9. https://doi.org/10.1016/j.ijhydene.2009.11.090.

[4] Yilmaz IT, Gumus M. Effects of hydrogen addition to the intake air on performance and emissions of common rail diesel engine. Energy 2018;142:1104–13. https://doi.org/10.1016/j.energy.2017.10.018.

[5] Sáinz D, Diéguez PM, Sopena C, Urroz JC, Gandía LM. Conversion of a commercial gasoline vehicle to run bi-fuel (hydrogen-gasoline). Int J Hydrogen Energy 2012;37:1781–9. https://doi.org/10.1016/j.ijhydene.2011.10.046.

[6] Sáinz D, Diéguez PM, Urroz JC, Sopena C, Guelbenzu E, Pérez-Ezcurdia A, et al. Conversion of a gasoline engine-generator set to a bi-fuel (hydrogen/gasoline) electronic fuel-injected power unit. Int J Hydrogen Energy 2011;36:13781–92. https://doi.org/10.1016/j.ijhydene.2011.07.114.

[7] Navale SJ, Kulkarni RR, Thipse SS. An experimental study on performance, emission and combustion parameters of hydrogen fueled spark ignition engine with the timed manifold injection system. Int J Hydrogen Energy 2017;42:8299–309. https://doi.org/10.1016/j.ijhydene.2017.01.059.

[8] Karim GA, Wierzba I, Al-Alousi Y. Methane-hydrogen mixtures as fuels.

Int J Hydrogen Energy 1996;21:625–31. https://doi.org/10.1016/0360-3199(95)00134-4.

[9] Ceper BA, Birsen EB, Akansu SO, Kahraman N. Experimental Study Of Hydrogen In Internal Combustion Engines. Clean Technol 2009 Bioenergy, Renewables, Storage, Grid, Waste Sustain 2009;3:191–4.

[10] Huang Z, Liu B, Zeng K, Huang Y, Jiang D, Wang X, et al. Combustion characteristics and heat release analysis of a spark-ignited engine fueled with natural gas-hydrogen blends. Energy and Fuels 2007;21:2594–9. https://doi.org/10.1021/ef0701586.

[11] Ma F, Wang M, Jiang L, Chen R, Deng J, Naeve N, et al. Performance and emission characteristics of a turbocharged CNG engine fueled by hydrogen-enriched compressed natural gas with high hydrogen ratio. Renew Energy 2010;35:6438–47. https://doi.org/10.1016/j.ijhydene.2010.03.111.

[12] Rakopoulos CD, Scott MA, Kyritsis DC, Giakoumis EG. Availability analysis of hydrogen/natural gas blends combustion in internal combustion engines. Energy 2008;33:248–55. https://doi.org/10.1016/j.energy.2007.05.009.

[13] Navarro E, Leo TJ, Corral R. CO2 emissions from a spark ignition engine operating on natural gas-hydrogen blends (HCNG). Appl Energy 2013;101:112–20. https://doi.org/10.1016/j.apenergy.2012.02.046.

[14] Hu E, Huang Z, Liu B, Zheng J, Gu X. Experimental study on combustion characteristics of a spark-ignition engine fueled with natural gas-hydrogen blends combining with EGR. Int J Hydrogen Energy 2009;34:1035–44. https://doi.org/10.1016/j.ijhydene.2008.11.030.

[15] Li Y, Bi M, Li B, Zhou Y, Gao W. Effects of hydrogen and initial pressure on flame characteristics and explosion pressure of methane/hydrogen fuels. Fuel 2018;233:269–82. https://doi.org/10.1016/j.fuel.2018.06.042.

[16] Zhou JH, Cheung CS, Leung CW. Combustion and Emission of a Compression Ignition Engine Fueled with Diesel and Hydrogen-Methane

Mixture 2013;7:112–7.

[17] Mansor MRA, Abbood MM, Mohamad TI. The influence of varying hydrogen-methane-diesel mixture ratio on the combustion characteristics and emissions of a direct injection diesel engine. Fuel 2017;190:281–91. https://doi.org/10.1016/j.fuel.2016.11.010.

[18] Dimitriou P, Tsujimura T. A review of hydrogen as a compression ignition engine fuel. Int J Hydrogen Energy 2017;42:24470–86. https://doi.org/10.1016/j.ijhydene.2017.07.232.

[19] Avadhanula VK, Lin C Sen, Witmer D, Schmid J, Kandulapati P. Experimental study of the performance of a stationary diesel engine generator with hydrogen supplementation. Energy and Fuels 2009;23:5062–72. https://doi.org/10.1021/ef900311w.

[20] Yoon W, Park J. Parametric study on combustion characteristics of virtual HCCI engine fueled with methane–hydrogen blends under low load conditions. Int J Hydrogen Energy 2019;44:15511–22. https://doi.org/10.1016/j.ijhydene.2019.04.137.

[21] Mariani A, Unich A, Minale M. Methane / Hydrogen Blends in Controlled Auto Ignition Engines with EGR : Evaluation of NOx Emissions 2019;74:301–6. https://doi.org/10.3303/CET1974051.

[22] Wong YK, Karim GA. An analytical examination of the efects of hydrogen addition on cyclic variations in homogeneously charged compression – ignition engines. Int J Hydrogen Energy 2000;25:1217–24.

[23] Nagalingam B, Duebel F, Schmillen K. Performance study using natural gas, hydrogen-supplemented natural gas and hydrogen in AVL research engine. Int J Hydrogen Energy 1983;8:715–20.

[24] Khasawneh H, Saidan MN, Al-Addous M. Utilization of hydrogen as clean energy resource in chlor-alkali process. Energy Explor Exploit 2019;37:1053–72. https://doi.org/10.1177/0144598719839767.

[25] Fuel Cells and Hydrogen 2 Joint Undertaking. HYDROGEN ROADMAP

EUROPE. A Sustainable Pathway for the European Energy Transition. Belgium: 2019. https://doi.org/10.2843/249013.

[26] Owen N. Roads2Hycom - Fuel Cells and Hydrogen in a Sustainable Energy Economy 2009:122.

[27] Moreno F, Muñoz M, Arroyo J, Magén O, Monné C, Suelves I. Efficiency and emissions in a vehicle spark ignition engine fueled with hydrogen and methane blends. Int J Hydrogen Energy 2012;37:11495–503. https://doi.org/10.1016/j.ijhydene.2012.04.012.

[28] Verhelst S, Maesschalck P, Rombaut N, Sierens R. Increasing the power output of hydrogen internal combustion engines by means of supercharging and exhaust gas recirculation. Int J Hydrogen Energy 2009;34:4406–12. https://doi.org/10.1016/j.ijhydene.2009.03.037.

[29] White CM, Steeper RR, Lutz AE. The hydrogen-fueled internal combustion engine: a technical review. Int J Hydrogen Energy 2006;31:1292–305. https://doi.org/10.1016/j.ijhydene.2005.12.001.

[30] Das LM. Hydrogen engines: a view of the past and a look into the future. Int J Hydrogen Energy 1990;15.

[31] Diéguez PM, Urroz JC, Marcelino-Sádaba S, Pérez-Ezcurdia A, Benito-Amurrio M, Sáinz D, et al. Experimental study of the performance and emission characteristics of an adapted commercial four-cylinder spark ignition engine running on hydrogen-methane mixtures. Appl Energy 2014;113:1068–76. https://doi.org/10.1016/j.apenergy.2013.08.063.

[32] Ma F, Wang M, Jiang L, Deng J, Chen R, Naeve N, et al. Performance and emission characteristics of a turbocharged spark-ignition hydrogen-enriched compressed natural gas engine under wide open throttle operating conditions. Int J Hydrogen Energy 2010;35:12502–9. https://doi.org/10.1016/j.ijhydene.2010.08.053.

[33] Huang Z, Liu B, Zeng K, Huang Y, Jiang D, Wang X, et al. Experimental study on engine performance and emissions for an engine fueled with natural gas-hydrogen mixtures. Energy and Fuels 2006;20:2131–6.

https://doi.org/10.1021/ef0600309.

[34] Ma F, Wang Y, Liu H, Li Y, Wang J, Zhao S. Experimental study on thermal efficiency and emission characteristics of a lean burn hydrogen enriched natural gas engine. Int J Hydrogen Energy 2007;32:5067–75. https://doi.org/10.1016/j.ijhydene.2007.07.048.

[35] Blarigan P Van, Keller JO. A hydrogen fuelled internal combustion engine designed for single speed/power operation. Int J Hydrogen Energy 1998;23:603–9.

[36] Yan F, Xu L, Wang Y. Application of hydrogen enriched natural gas in spark ignition IC engines: from fundamental fuel properties to engine performances and emissions. Renew Sustain Energy Rev 2018;82:1457–88. https://doi.org/10.1016/j.rser.2017.05.227.

[37] Moreno F, Arroyo J, Muñoz M, Monné C. Combustion analysis of a spark ignition engine fueled with gaseous blends containing hydrogen. Int J Hydrogen Energy 2012;37:13564–73. https://doi.org/10.1016/j.ijhydene.2012.06.060.

[38] Wang Y, Zhang X, Li C, Wu J. Experimental and modeling study of performance and emissions of SI engine fueled by natural gas-hydrogen mixtures. Int J Hydrogen Energy 2010;35:2680–3. https://doi.org/10.1016/j.ijhydene.2009.04.048.

[39] Hora TS, Agarwal AK. Experimental study of the composition of hydrogen enriched compressed natural gas on engine performance, combustion and emission characteristics. Fuel 2015;160:470–8. https://doi.org/10.1016/j.fuel.2015.07.078.

[40] Kahraman N, Çeper B, Akansu SO, Aydin K. Investigation of combustion characteristics and emissions in a spark-ignition engine fuelled with natural gas-hydrogen blends. Int J Hydrogen Energy 2009;34:1026–34. https://doi.org/10.1016/j.ijhydene.2008.10.075.

[41] Reyes M, Tinaut F V., Melgar A, Pérez A. Characterization of the combustion process and cycle-to-cycle variations in a spark ignition

engine fuelled with natural gas/hydrogen mixtures. Int J Hydrogen Energy 2016;41:2064–74. https://doi.org/10.1016/j.ijhydene.2015.10.082.

[42] Guy Maisonnier, Perrin J, Steinberger-wilckens R, Trümper SC. “ European Hydrogen Infrastructure Atlas ” and “ Industrial Excess Hydrogen Analysis ” PART II : Industrial surplus hydrogen and markets and production. Roads2HyCom 2007:86.

[43] Ball M, Wietschel M. The Hydrogen Economy. Opporunities and Challenges. New York: Cambridge University Press; 2009.

[44] Guy Maisonnier, Perrin J, Steinberger-wilckens R, Trümper SC. “ European Hydrogen Infrastructure Atlas ” and “ Industrial Excess Hydrogen Analysis ” PART II : Industrial surplus hydrogen and markets and production. Roads2HyCom 2007:86. https://doi.org/10.1088/1367-2630/9/4/092.

[45] Remus R, Aguado Monsonet MA, Roudier S, Sancho LD. Best Available Techniques (BAT) Reference Document for Iron and Steel Production. vol. BREF-IS. 2013. https://doi.org/10.2791/97469.

[46] Roy MM, Tomita E, Kawahara N, Harada Y, Sakane A. Performance and emission comparison of a supercharged dual-fuel engine fueled by producer gases with varying hydrogen content. Int J Hydrogen Energy 2009;34:7811–22. https://doi.org/10.1016/j.ijhydene.2009.07.056.

[47] Yáñez M, Ortiz A, Brunaud B, Grossmann IE, Ortiz I. Contribution of upcycling surplus hydrogen to design a sustainable supply chain: The case study of Northern Spain. Appl Energy 2018;231:777–87. https://doi.org/10.1016/j.apenergy.2018.09.047.

[48] Corporation USS. Clean Coke Oven Gas. Safety Data Sheet (SDS). Exposure 2010;82493:1–8.

[49] Roy MM, Tomita E, Kawahara N, Harada Y, Sakane A. Performance and emissions of a supercharged dual-fuel engine fueled by hydrogen-rich coke oven gas. Int J Hydrogen Energy 2009;34:9628–38. https://doi.org/10.1016/j.ijhydene.2009.09.016.

[50] Roy MM, Tomita E, Kawahara N, Harada Y, Sakane A. Comparison of performance and emissions of a supercharged dual-fuel engine fueled by hydrogen and hydrogen-containing gaseous fuels. Int J Hydrogen Energy 2011;36:7339–52. https://doi.org/10.1016/j.ijhydene.2011.03.070.

[51] Feng H, Zhang W, Zhang J, Wang X, Zhang X. Availability analysis of a coke oven gas fueled spark ignition engine. Int J Hydrogen Energy 2018;43:1835–45. https://doi.org/10.1016/j.ijhydene.2017.11.125.

[52] Szwaja S. Hydrogen rich gases combustion in the IC engine. J KONES Powertrain Transp 2009;16:448–54.

[53] Szwaja S. Dilution of fresh charge for reducing combustion knock in the internal combustion engine fueled with hydrogen rich gases. Int J Hydrogen Energy 2018. https://doi.org/10.1016/j.ijhydene.2018.10.134.

[54] He H, Yao D, Wu F. A reduced and optimized kinetic mechanism for coke oven gas as a clean alternative vehicle fuel. J Zhejiang Univ A 2017;18:511–30. https://doi.org/10.1631/jzus.A1600636.

[55] Naeve N, He Y, Deng J, Wang M, Ma F. Waste Coke Oven Gas Used as a Potential Fuel for Engines. SAE Int 2011. https://doi.org/10.4271/2011-01-0920.

[56] Jian L, Chau KT. Design and analysis of a magnetic-geared electronic-continuously variable transmission system using finite element method. Prog Electromagn Res 2010;107:47–61.

[57] CVT Corp. Ind Most Powerful Mech CVTs 2016. https://www.cvtcorp.com/main.php?i=15 (accessed December 7, 2019).

[58] Sáinz Casas D. Adaptación de un motor de combustión interna alternativo de gasolina para su funcionamiento con hidrógeno como combustible. Aplicaciones energética y de automoción. Universidad Pública de Navarra, 2014.

[59] Heywood JB. Internal combustion engine fundamentals. 1988.

[60] Karim GA. Hydrogen as a spark ignition engine fuel. Int J Hydrogen

Energy 2003;28:569–77. https://doi.org/10.1016/S0360-3199(02)00150-7.

[61] Wang J, Wei Z, Zhang M, Huang Z. A review of engine application and fundamental study on turbulent premixed combustion of hydrogen enriched natural gas. Sci China Technol Sci 2014;57:445–51. https://doi.org/10.1007/s11431-014-5471-y.

[62] Liu G, Zhou J, Wang Z, Liu J. Study of Laminar Flame Speeds of Premixed Coke Oven Gas Flame Using Kinetic Simulation. 11th China-Japan-Korea Student Symp., Hangzhou: 2017.

[63] D. McNaught A, Wilkinson A. IUPAC Compendium of Chemical Terminology. Gold Book. 2nd ed. 1997.

[64] Di Sarli V, Di Benedetto A. Laminar burning velocity of hydrogen-methane/air premixed flames. Int J Hydrogen Energy 2007;32:637–46. https://doi.org/10.1016/j.ijhydene.2006.05.016.

[65] Donohoe N, Heufer A, Metcalfe WK, Curran HJ, Davis ML, Mathieu O, et al. Ignition delay times, laminar flame speeds, and mechanism validation for natural gas/hydrogen blends at elevated pressures. Combust Flame 2014;161:1432–43. https://doi.org/10.1016/j.combustflame.2013.12.005.

[66] Diéguez PM, Urroz JC, Sáinz D, Machin J, Arana M, Gandía LM. Characterization of combustion anomalies in a hydrogen-fueled 1.4 L commercial spark-ignition engine by means of in-cylinder pressure, block-engine vibration, and acoustic measurements. Energy Convers Manag 2018;172:67–80. https://doi.org/10.1016/j.enconman.2018.06.115.

[67] Mehra RK, Duan H, Juknelevičius R, Ma F, Li J. Progress in hydrogen enriched compressed natural gas (HCNG) internal combustion engines - A comprehensive review. Renew Sustain Energy Rev 2017;80:1458–98. https://doi.org/10.1016/j.rser.2017.05.061.

[68] Sun Y, Yu X, Dong W, Tang Y. Effects of hydrogen direct injection on engine stability and optimization of control parameters for a combined injection engine. Int J Hydrogen Energy 2018;43:6723–33. https://doi.org/10.1016/j.ijhydene.2018.02.033.

[69] Ceper BA, Akansu SO, Kahraman N. Investigation of cylinder pressure for H2/CH4 mixtures at different loads. Int J Hydrogen Energy 2009;34:4855–61. https://doi.org/10.1016/j.ijhydene.2009.03.039.

[70] Park C, Kim C, Choi Y, Won S, Moriyoshi Y. The influences of hydrogen on the performance and emission characteristics of a heavy duty natural gas engine. Int J Hydrogen Energy 2011;36:3739–45. https://doi.org/10.1016/j.ijhydene.2010.12.021.

[71] Ma F, Wang J, Wang Y, Wang Y, Li Y, Liu H, et al. Influence of different volume percent hydrogen/natural gas mixtures on idle performance of a CNG engine. Energy and Fuels 2008;22:1880–7. https://doi.org/10.1021/ef7006485.

[72] Mehra RK, Duan H, Luo S, Rao A, Ma F. Experimental and artificial neural network (ANN) study of hydrogen enriched compressed natural gas (HCNG) engine under various ignition timings and excess air ratios. Appl Energy 2018;228:736–54. https://doi.org/10.1016/j.apenergy.2018.06.085.

[73] Hoekstra RL, Van Blarigan P, Mulligan N. NOx emissions and efficiency of hydrogen, natural gas, and hydrogen/natural gas blended fuels. SAE Tech Pap 1996. https://doi.org/10.4271/961103.

[74] Shudo T, Shimamura K, Nakajima Y. Combustion and emissions in a methane DI stratified charge engine with hydrogen pre-mixing. JSAE Rev 2000;21:3–7. https://doi.org/10.1016/S0389-4304(99)00061-2.

[75] Alrazen HA, Ahmad KA. HCNG fueled spark-ignition (SI) engine with its effects on performance and emissions. Renew Sustain Energy Rev 2018;82:324–42. https://doi.org/10.1016/j.rser.2017.09.035.

[76] Yan F, Xu L, Wang Y. Application of hydrogen enriched natural gas in spark ignition IC engines: from fundamental fuel properties to engine performances and emissions. Renew Sustain Energy Rev 2018;82:1457–88. https://doi.org/10.1016/j.rser.2017.05.227.

[77] Akansu SO, Kahraman N, Çeper B. Experimental study on a spark

ignition engine fuelled by methane-hydrogen mixtures. Int J Hydrogen Energy 2007;32:4279–84. https://doi.org/10.1016/j.ijhydene.2007.05.034.

[78] Bauer CG, Forest TW. Effect of hydrogen addition on the performance of methane-fueled vehicles. Part I: effect on S.I. engine performance. Int J Hydrogen Energy 2001;26:55–70. https://doi.org/10.1016/S0360-3199(00)00067-7.

[79] Wu L, Kobayashi N, Li Z, Huang H. Experimental study on the effects of hydrogen addition on the emission and heat transfer characteristics of laminar methane diffusion flames with oxygen-enriched air. Int J Hydrogen Energy 2016;41:2023–36. https://doi.org/10.1016/j.ijhydene.2015.10.132.

[80] Xu J, Zhang X, Liu J, Fan L. Experimental study of a single-cylinder engine fueled with natural gas-hydrogen mixtures. Int J Hydrogen Energy 2010;35:2909–14. https://doi.org/10.1016/j.ijhydene.2009.05.039.

[81] Açikgöz B, Çelik C, Soyhan HS, Gökalp B, Karabağ B. Emission characteristics of an hydrogen-CH4 fuelled spark ignition engine. Fuel 2015;159:298–307. https://doi.org/10.1016/j.fuel.2015.06.043.

[82] Akansu SO, Dulger Z, Kahraman N, Veziroğlu TN. Internal combustion engines fueled by natural gas - Hydrogen mixtures. Int J Hydrogen Energy 2004;29:1527–39. https://doi.org/10.1016/j.ijhydene.2004.01.018.